GROUND-BASED OBSERVATIONS OF MARS AND VENUS WATER VAPOR DURING 1972 AND 1973

E. S. BARKER

University of Texas, McDonald Observatory, Fort Davis, Tex., U.S.A.

Abstract. The Venus water vapor line at 8197.71 Å has been monitored at several positions on the disk of Venus and at phase angles between 22° and 91°. Variations in the abundance have been found with both position and time. The total two-way transmission has varied from less than 5 to 77 μ of water vapor. Comparisons will be made between the water vapor abundances, presence of UV features, and the CO_2 abundances determined from near simultaneous observations of CO_2 bands at the same positions on the disk of Venus.

The amount of Martian atmospheric water vapor has been monitored during the past two years at McDonald Observatory using the échelle coudé scanner of the 272 cm reflector. Two periods of the Martian year have been monitored. The first period was during and after the great 1971 dust storm ($L_s = 280°$ to 20° or summer in the southern hemisphere). The results obtained will be compared to the Mariner 9 IRIS and Mars 3 observations made during the same period.

During the second period ($L_s = 124°$ to 266°) observations were made to follow the seasonal latitudinal and diurnal changes in the water vapor abundance in the Martian atmosphere. The water vapor abundance declines from a maximum of 20–35 μm at $L_s = 125°$ to the 5–15 μm level at $L_s = 180°$. Then it remained relatively constant until $L_s = 250°$ when the increase to 20–25 μm occurred in the southern latitudes. Studies of the latitudinal and diurnal water vapor distributions indicate the location of maximum and minimum abundances for this season are positively correlated with surface temperature variations.

1. Introduction

As part of the continuing planetary observational program at McDonald Observatory, the several lines in the 8200 Å water vapor band are monitored as frequently as possible to study variations in the observed abundance of Venus water vapor 'above the clouds', and to follow the seasonal and spatial variations in the water vapor abundance in Martian atmosphere. Both 2 Å mm^{-1} spectrographic plates and photoelectric scanner observations have been taken since completion of the 107-in. (272 cm) telescope in the spring of 1969. Other papers presented at this IAU meeting cover the historical evolution of the search for water vapor in planetary atmospheres (Schorn and Barker, 1973; Traub and Carleton, 1973). This paper will describe only the McDonald results obtained during 1972 and up to August 15, 1973.

2. Instrumentation and Reductions

Photoelectric spectrum scans have been made using the rapid scanner at the coudé focus of the 107-in. (272 cm) telescope which has an image scale of 2.3″ mm^{-1}, ideally suited for spatial resolution on planetary disks. We have used essentially the same system for the Mars and Venus observations; a 79 groove per mm échelle grating in double pass which gives a very high dispersion of 8 mm $Å^{-1}$ at 8200 Å. The only difference is the choice of slit widths used which define the resolution obtained. With 200 μm slits, a final resolution of about 30 mÅ or 275000 at 8200 Å (FWHM)

Woszczyk and Iwaniszewska (eds.), Exploration of the Planetary System, 203–222.

is attainable; similarly, 400 μm slits give about 60 mÅ. The entire system is described in more detail by Tull (1972) and Wells (1972).

RCA GaAs (31034 and 31034 A) photomultipliers have made possible these high resolution and photometrically accurate scans. Their high quantum efficiency (10 to 20% at 8200 Å coupled with the low dark count of 2 counts/s at dry ice temperatures) makes it possible to obtain high quality photoelectric scans of a single line within 10 min for Venus and 40 min for Mars. Scans can be made about 50 times faster now than when the échelle scanner was put into operation two years ago. Different slit widths or effective resolutions have been used to compensate for or take advantage of the quantum efficiency of the photomultiplier available at the time. In general, all the Venus scans have a resolution (FWHM) of 30 mÅ and the Mars scans have 60 mÅ. The Mars scans obtained since the beginning of June, 1973, are an exception and are at the higher resolution. This was necessitated because the Doppler shift decreased to less than 0.25 Å and terrestrial humidity increased during the summer months at McDonald Observatory.

Most strong water lines in the 8200 Å band are contaminated to some degree by weak Fraunhofer lines primarily due to CN transitions. All usable water lines (i.e., free from major blends and having laboratory line strengths) have been observed on Mercury, as a source of variable Doppler shift, to look for 'hidden' Fraunhofer lines. Lines at 8141, 8193, and 8256 Å are so seriously blended that they are not usable for future studies. Weak lines in the wings of 8176, 8189, and 8197 Å have been measured and can be used if the solar component of the Doppler shift does not place them at the Doppler shifted wavelengths of Mars and Venus water lines. The work presented in this paper uses primarily the line at 8176.9 Å for Mars and the line at 8197.7 Å for Venus.

An image rotator allowed the slit of the spectrograph to be oriented with respect to the intensity equator on Venus or Mars and the Martian north–south direction. On a few occasions a decker was used to shorten the slit to cover only part of the planet, but usually the slit length was just slightly larger than the planet's diameter to minimize the amount of sky background. The counting ratio between the planet-plus-sky and sky was monitored several times during each scan. With this ratio the appropriate amount of sky background was subtracted from each planet scan by using a sky or solar scan of the same wavelength region obtained on the same day.

Each photoelectric scan is processed through several steps to remove effects of sky background, dark count level, and vignetting in the échelle system. The final plot of the spectrum consists of data points representing the summation of the forward and reverse scans and a smooth curve through these data points which has been drawn by the computer as a result of a Fast Fourier Transform smoothing and interpolating operation on the data. All equivalent widths are measured with respect to such a smoothed curve. The local continuum curve has been transferred from a solar scan of similar water content taken on the same day. Attempts have been made to produce a synthetic solar spectrum scan to calculate a ratio spectrum with the planetary scan leaving only the planetary component of the water line. Both methods have the same

major source of error (namely the placement of the continuum level), and we feel that we are adding an additional source of error by trying to produce a solar scan having identical water content and instrumental resolution.

The digital form of the photoelectric data makes computer processing of data almost routine and processing presently is being carried out within a few days after the observation using an IBM 1800 computer at McDonald Observatory. Lack of manpower is the only reason for not always producing reduced spectra immediately after an observation, although we do so when the occasion warrants. Compared to the former time lag of weeks and the necessary travel to a microdensitometer to reduce regular photographic plates, our present system is far superior and, most important, we can modify our observing program on a day to day basis to best utilize available observing time.

3. Venus Observations

The 107-in. échelle-coudé scanner has proved to be well suited for spatial studies of Venus water vapor, mostly because of its speed, a prime requirement for spatial studies requiring good seeing over a long period of time. With a resolution of 30 mÅ

TABLE I

Physical data for Venus H_2O observations

Date	$\Delta\lambda$ (Å)	i (°)	Diameter (arcsec)	CO_2	UV
8/24/72	+0.369	91.0	24.4	+	+
9/23/72	+0.350	74.3	18.4	+	+
9/24/72	+0.350	73.8	18.2	+	+
9/26/72	+0.347	73.3	17.9	+	+
9/29/72	+0.344	71.4	17.5	+	+
11/25/72	+0.262	47.2	12.7		
11/30/72	+0.253	45.2	12.5		
12/01/72	+0.251	42.9	12.4		
12/12/72	+0.231	40.4	11.9		
12/13/72	+0.229	40.0	11.8		
12/14/72	+0.227	39.6	11.8		
12/16/72	+0.225	38.9	11.7		
6/05/73	−0.139	21.2	10.2		
6/14/73	−0.164	24.8	10.4		?
6/16/73	−0.169	25.6	10.4		?
6/17/73	−0.171	26.0	−10.4		?
7/07/73	−0.221	34.1	11.0	+	?
7/08/73	−0.223	34.5	11.0		?
8/03/73	−0.276	45.1	11.3		?
8/04/73	−0.278	45.5	11.4		?
8/10/73	−0.288	47.9	11.7	+	?
8/12/73	−0.291	48.7	11.8	+	?
8/14/73	−0.294	49.5	12.7	+	?
8/15/73	−0.296	49.9	12.8	+	?

(FWHM) which is better than the resolution of a 2 Å mm^{-1} spectrographic plate, we can obtain a water line scan in 15 min, compared to a plate exposure of one hour. This means we can observe at many locations on the disk of Venus during a few hours of good seeing.

The physical data for the Venus scanner observations of the 8197.7 Å and 8176.9 Å lines are summarized in Table I. Table I contains the physical data pertinent to Venus observations and indicates that phase angle coverage is fairly good between 20° and 90°. It is difficult to observe near phase angles of 0° and 180° because of the small Doppler shifts involved. Only those observations reported by Traub and Carleton (1973, 1974) have been made at phase angles greater than 120°. Schorn *et al.* (1969) presented observations over phase angles of 52° to 92°. The scanner resolution and terrestrial water vapor limit the useful Doppler shift range to greater than ± 0.15 Å which corresponds to approximate phase angle limits of $20° < i < 150°$.

Total abundances ($\eta\omega$) for a two-way transmission through the Venus atmosphere were calculated on assumptions of an effective pressure of 100 mb and a temperature of 250 K. The H_2O line strengths (Farmer, 1971) at 250 K were used to calculate total abundances from the observed equivalent widths. The internal error involved in a scan is around ± 5 μm of precipitable H_2O.

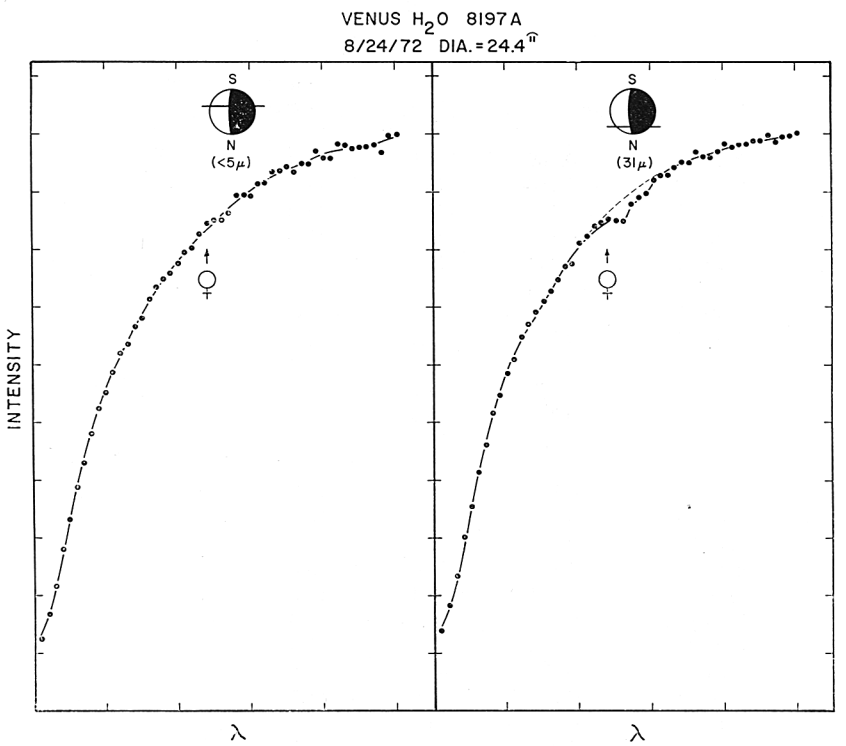

Fig. 1. The position of 8197 Å water vapor line on Venus is indicated by the ♀ symbol. The slit position is shown in the small insert.

https://doi.org/10.1017/S0074180900025456 Published online by Cambridge University Press

Putting the amounts of <5 to 77 μm of water vapor in perspective with previous measurements, they fall between the total disk values of Fink *et al.* (1972) who found 1.6 μm for the water bands at 1.4, 1.9 and 2.7 μ, and those found by Schorn *et al.* (1969) and Owen (1968) of <64 to 120 μm using several lines in the 8200 Å band.

Variability of amount of water vapor with phase angle and position on the disk is illustrated in Figures 1 and 2. Figure 1 shows the red wing of the 8197 Å water line for two different spectrograph slit positions, S1/4 and N3/4. The slit in most cases was placed parallel to the intensity equator and the N–S notation is for convenience only to indicate a position N or S of the intensity equator. It does not refer to the actual N–S direction on Venus. An upper limit of 5 μm at the S1/4 position contrasts with the easily detectable amount of 30 μm at the N3/4 position. Scans shown in Figure 2 again graphically show that we can find different amounts of water vapor at different locations on the disk. The 56 μm in the equator scan is the largest amount detected during the August, 1972, through August, 1973, period and would have barely been detectable on 2 Å mm^{-1} spectrographic plates. Comparable amounts have been seen on many spectrographic plates taken at McDonald since 1967, but the spectrographic plates lacked the resolution and photometric accuracy needed to detect smaller amounts.

A summary of spatial distribution data is presented in Figure 3 with various slit

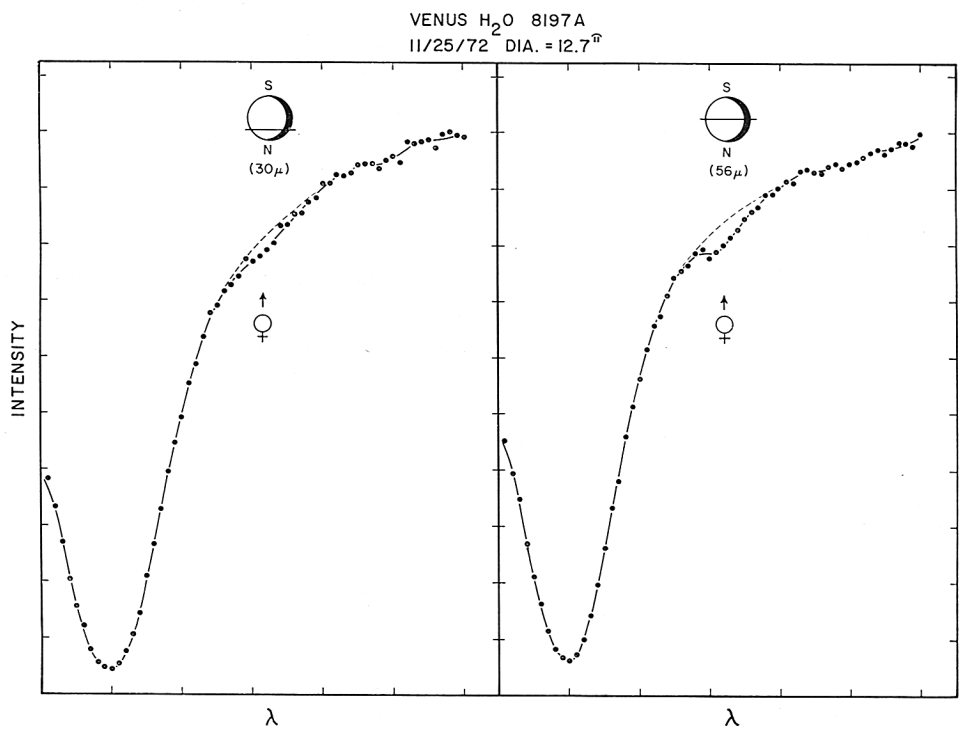

Fig. 2. The position of 8197 Å water vapor line on Venus is indicated by the ♀ symbol. The slit position is shown in the small insert.

https://doi.org/10.1017/S0074180900025456 Published online by Cambridge University Press

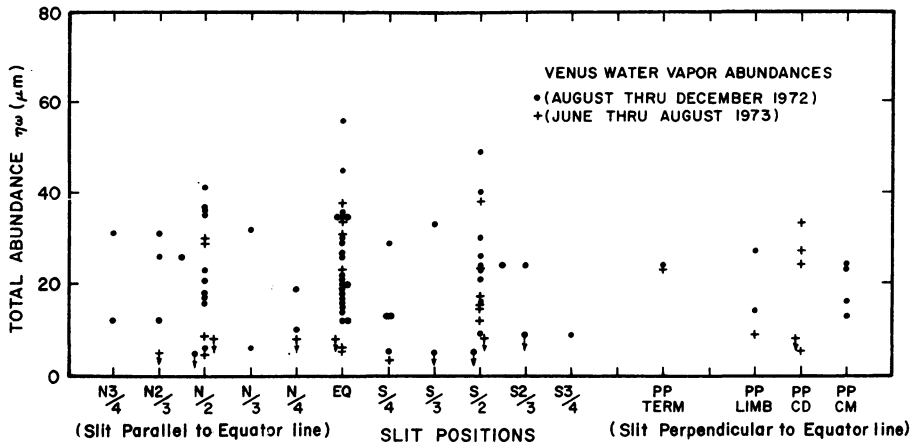

Fig. 3. Spacial distribution of water vapor determinations over the disk of Venus. Slit Positions: Parallel to intensity equator at various fractions of disk diameter toward poles; N3/4, N2/3, N/2, N/3, N/4, EQ, S/4, S/3, S/2, S2/3, S3/4. Perpendicular to intensity equator or pole to pole at various fractions of disk diameter; T designates terminator, CM – central meridian, CD – center of disk, L – limb; PP T/3, PP T/2, PP CM, PP C/3, PP CD, PP L/2, PP L/3.

positions explained in the caption. There does not seem to be any preferential location for high or low abundances. The detection limit (indicated by vertical arrows in Figure 3) was around 5 to 8 μm, a value frequently reached at various phase angles and points on the disk.

Variation of the equivalent width of a line as a function of phase angle can be used as a parameter in models to explain the vertical structure of cloud layering on Venus (Hunt, 1972a, b; Margolis and Hunt, 1973). In Figure 4 the 1972–73 observations of total water vapor abundance on Venus are plotted as a function of phase angle and/or time. Several points at one phase angle indicate abundance variations for various slit

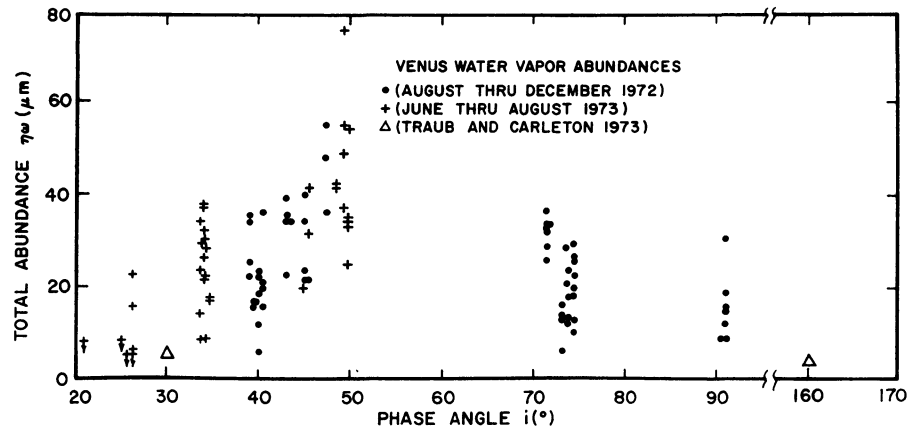

Fig. 4. Venus water vapor determinations on various dates or at different phase angles, *i*.

https://doi.org/10.1017/S0074180900025456 Published online by Cambridge University Press

positions on that day. A typical internal error bar is ± 5 μm; these have been left off the figure for clarity. Some scans exhibited no Venus water line at all and are indicated by vertical arrows representing an upper limit to the abundance for that scan.

No compelling correlation between phase angle and water vapor abundance is present in Figure 4; in fact, the large scatter at any one phase angle could suggest the conclusion that we are observing a random event. However, there is a possibility of preferential appearance of the larger abundances at intermediate phase angles 35°–90°. Observations of lower abundances at phase angles greater than 140° and less than 30° are consistent with the two observations of Traub and Carleton (1973, 1974) in which they report no line greater than 0.1 mÅ or a total abundance of 1 μm at $i = 1.56°$ and a detectable line of 0.5 mÅ or a total abundance of 5 μm at $i = 30°$. As indicated earlier, the Doppler shifts are small in these phase angle ranges ($i < 30°$, $i > 150°$) and may lead to large uncertainties in the measured equivalent widths of non-terrestrial water lines which are masked by strong telluric components only 0.1 Å away. Only observations with very high resolution (>250000) and dry terrestrial conditions can be used when

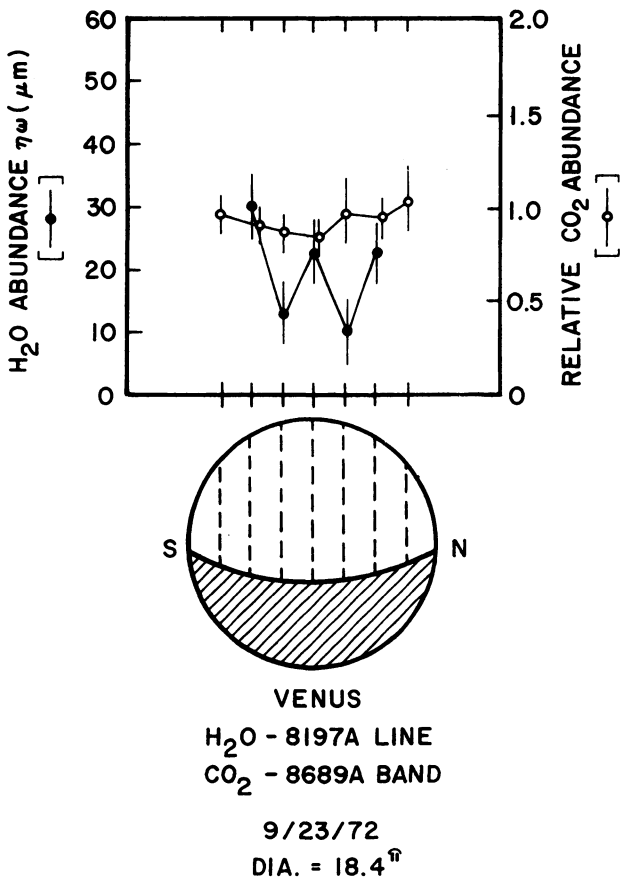

Fig. 5. Venus water vapor and CO_2 abundances for the same slit positions on September 23, 1972.

https://doi.org/10.1017/S0074180900025456 Published online by Cambridge University Press

the Doppler shifts are so small. Attempts will be made at McDonald in January of 1974 during our dry season to observe at phase angles greater than 150°. Since we will have a very large crescent (>40″), we hope to see any variations in the spatial distribution along the crescent similar to the changes of a factor of two or three noted in abundance during the 1972 inferior conjunction (Barker and Schorn, 1973).

As seen from Table I, it will be possible to intercompare the CO_2 and H_2O abundances and the ultraviolet (UV) features for several days during September, 1972. As a sample, Figure 5 shows the slit positions for H_2O and CO_2 abundance determinations made within hours on the same day. Note that CO_2 is relatively constant on this day whereas H_2O abundances vary by a factor of 3.

On this day the ultraviolet 'Y' feature was present on the disk, but offset to the south making any comparison with UV features difficult for slits placed parallel to the intensity equator. But high and low water vapor abundance values fall over both light and dark areas.

Note in Figure 6 that on this day the variations in CO_2 and H_2O abundances may

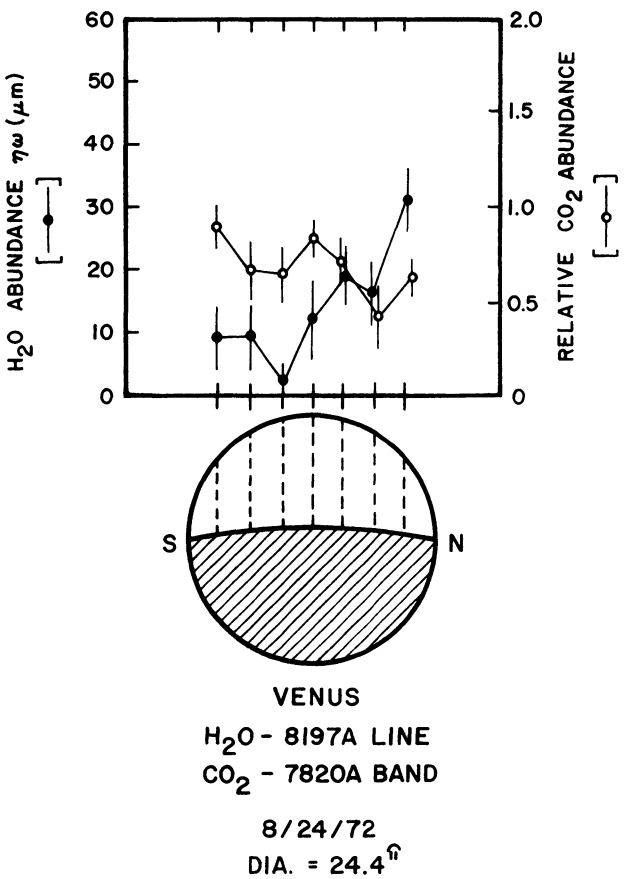

Fig. 6. Venus water vapor and CO_2 abundances for the same slit positions on August 24, 1972.

https://doi.org/10.1017/S0074180900025456 Published online by Cambridge University Press

be positively correlated. However, the systematic trends were of decreasing CO_2 and of increasing H_2O from south to north across the disk.

Young *et al.* (1973) have noted a four-day periodicity in the relative CO_2 absorption strength in their observations of the 8689 Å CO_2 band during September and early October of 1972. Similar observations were obtained at McDonald Observatory with the 107-in. (272 cm) and 82-in. (208 cm) coudé spectrographs (Schorn and Barker, 1973). The 107-in. data on the 7820 and 8700 Å CO_2 bands show a similar periodicity. Unfortunately, the coverage of the 8197 Å water vapor abundance during the same period of time was not as complete as the CO_2 data, being only four days out of 13. Detailed intercomparison between days and slit positions may reveal a slight periodicity, but the CO_2 photographic spectral data are not yet fully reduced.

The Venus water vapor observations during 1972–73 show quite conclusively a day-to-day abundance variation and also a significant abundance variation with position on the disk of Venus on any single day. Consequently, the level or altitude of line formation must change, consistent with vertical and/or horizontal movement of the altitude of 'tops' of the lower cloud deck.

4. Mars Observations

The search for Martian water vapor has long been pursued, with first spectrographic detection being obtained by Spinrad *et al.* (1963). Subsequently, further ground-based studies were presented by Schorn *et al.* (1967), Owen (1967, 1969), Schorn *et al.* (1969) Tull (1970), Barker *et al.* (1970), Barker (1971), Tull and Barker (1972), and Larson (1973). We also have *in situ* measurements made by Mariner 9 and Mars 2 and 3 reported by Hanel *et al.* (1972), Kunde (1973), Moroz and Ksanfomaliti (1972), and Moroz and Petrov (1973). Despite all these observations, there still remain parts of the Martian year which have not been covered observationally, because a period of 15 years is required to fully observe from the Earth all seasons on Mars. Also we have no *a priori* reason to believe that the weather on Mars is the same every year. The great dust storm of 1971–1972 is an obvious example which affected the water vapor content detected in the Martian atmosphere both during and after the storm.

This paper presents two results: (1) additional data obtained during the 1971–72 apparition after dissipation of the great dust storm; and (2) data obtained in the 1972–74 apparition through August, 1973, which cover a seasonal period ($150° < L_s < 230°$) which had not previously been observed. The later results bear on interesting questions: (a) Does the water vapor disappear between the northern hemisphere summer-fall season and the reappearance of larger abundance values (20–50 μm) during the southern hemisphere late summer season? (b) If the water does not disappear, how is the transition made between hemispheres and where is the water vapor located spatially with respect to aerographic latitude and diurnal distribution of the water vapor.

4.1. Water vapor observations during and after the great dust storm of 1971

Tull and Barker (1972) presented 1971–72 data in preliminary form. This section is

TABLE II

Mars H_2O abundances for the 1971–72 apparition

L_s	Amount (μm)	Location	Reference
232°	20	Total Disk	Larson (1973)
293°	10–25	SSolar Rev 20	Hanel *et al.* (1972)
297°	5–20	SPC Rev 30	Hanel *et al.* (1972)
314°	10–20	SSolar Rev 92	Hanel *et al.* (1972)
321°	5–20	SPC Rev 116	Hanel *et al.* (1972)
336°	5–15	SSolar Rev 174	Hanel *et al.* (1972)
270–360°	8	NPC	Kunde (1973)
60°	20–30	Northern hemisphere	Kunde (1973)
352°	1–3	S–N track $\pm 50°$ lat.	Moroz (1972)
358°	20	Equatorial	Moroz (1972)
286°	16.5	PPCM	Tull (1972)
285°	12.0	PPCM	Tull (1972)
286°	10.5	PPCM	Tull (1972)
288°	13.5	PPCM	Tull (1972)
299°	13.0	PPCM	Tull (1972)
314°	18.25	PPCM	Tull (1972)
316°	7.5	EQ	Tull (1972)
324°	10.75	PPCM	Tull (1972)
327°	7.0	PPCM	Tull (1972)
332°	6.0	PPCM	Tull (1972)
348°	13.0	PPCM	Tull (1972)
350°	13.5	PPCM	Tull (1972)
352°	14.0	PPCM	Tull (1972)
353°	15.0	PPCM	Tull (1972)
353°	16.5	PPCM	Tull (1972)
11°	9.3	PPCM	This paper
21°	5.0	PPCM	This paper

devoted to combining their data with a few additional ground-based observations made by Larson (1973) and with spacecraft determinations made by Mars 2 and 3 and by Mariner 9.

A summary of 1971–72 observations appears in Table II and Figure 7 in which cross-hatched areas refer to previous determinations and other points are identified in the caption. An obvious conclusion is that after the 1971 dust storm the reappearance of atmospheric water vapor during the southern summer season ($270° < L_s < 360°$) was different from the usual reappearance pattern. Two primary reasons have been advanced by Hanel *et al.* (1972) and others for the much lower abundance (5–20 μm vs 20–50 μm) during the great dust storm summer: (1) a larger amount of water may have been trapped in the northern cap (since the north polar hood extended further south than usual); and/or (2) the release of water vapor in the southern hemisphere may

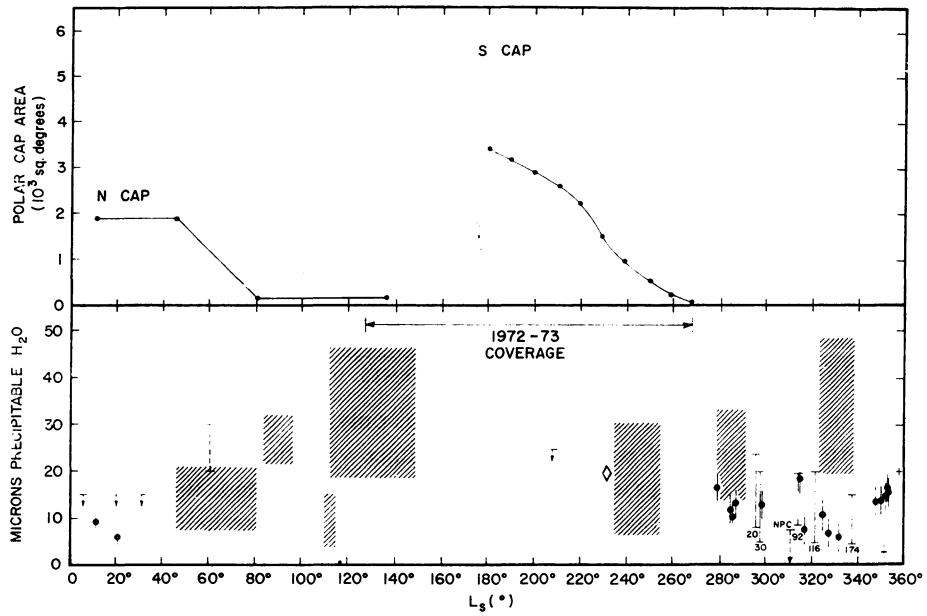

Fig. 7. Mars H_2O abundances for the 1971–72 apparition. The cross-hatched areas refer to pre-1971 determinations. ◇ Larson (1973); | Mariner 9 data from Hanel *et al.* (1972) with the revolution number attached to the bar; ¦ Mariner 9 data from Kunde (1973); + Mars 3 data from Moroz and Ksanfomaliti (1972); ⧫ ground-based data from Tull and Barker (1972). Surface area of polar caps calculated from Baum and Martin (1973).

have been curtailed by the dust storm which occurred at a season preceding the time when water vapor would be expected to increase in the southern hemisphere (Barker *et al.*, 1970; Barker, 1971). This curtailment could be caused, for example, by adsorption on the dust particles or simply by a thick dust covering on moisture-laden soil.

Agreement among the three sets of data, ground-based (Tull and Barker, 1972), Mariner 9 (Hanel, 1972; Kunde, 1973), and Mars 3 (Moroz and Ksanfomaliti, 1972), is quite good and indicates that the higher spatial resolution spacecraft measurements were representative of the entire planetary atmosphere during the southern summer season in 1971–72.

The airborne observation at $L_s = 232°$ obtained near opposition by Larson (1973) was made before the onset of the major dust storm and before the period of time when the Doppler shift was large enough for ground-based observations. The value of 20 μm agrees with previous determination at this L_s by Barker *et al.* (1970) indicating that water vapor was beginning its normal reappearance in the southern spring season. The major dust storm commenced at an L_s of 263° and the atmospheric water vapor content observed above the dust during the storm and then subsequent to it was less than 15 to 25 μm throughout the remainder of the southern summer, instead of increasing to a maximum near $L_s = 330°$ as it did in 1969.

The single Mariner 9 data point of 20 to 30 μm at an $L_s = 60°$ (Kunde, 1973) during

the northern spring suggests that water vapor content had returned to normal by that time and no longer showed the effects of the dust storm.

Surface area of the polar caps has been calculated from data presented by Baum and Martin (1973) and Baum (1973) on the behavior of boundaries of polar caps since 1905. The standstill period for the north cap occurs between an L_s of 10° and 50°. Then the area decreases to the size of the permanent cap at $L_s = 80°$. Due to the eccentric boundary of the south cap, the standstill period is not as obvious and there appears to be a second standstill period between $L_s = 180°$ and 220°. Then the south cap retreats to its minimum size. Note that maximum water vapor abundance does not occur until the surface area of the north and south cap reaches a minimum value.

4.2. 1972–73 MARTIAN WATER VAPOR MEASUREMENTS

Starting in late November, 1972, when Mars was only 4.5″ diam, we have carried out a very extensive patrol of water vapor abundance variations on Mars. About 250 photoelectric scans or water vapor determinations have been made through August 15, 1973 providing an L_s coverage of $118° < L_s < 263°$ which has been indicated in Figure 7. Most important is the filling in of a completely unobserved range of L_s between 150° and 230° with spectra taken pole-to-pole along the Martian central meridian. By $L_s = 139°$ we were able to begin a study of latitudinal distribution of water vapor as the subsolar point moved southward into the southern hemisphere. Latitudinal spectra were taken with the slit placed parallel to the Martian equator at various fractions of the polar disk diameter from the equator such as N/2, S2/3. Diurnal observations of water vapor content were begun at an $L_s = 170°$. Diurnal data consist of spectral scans taken with the entrance slit parallel to the terminator and placed respectively near the termination, at the center of the disk, and near the limb. Terminator and limb scans were taken with the center of the slit 1.5″ in form of the visible terminator and limb and were made only when atmospheric conditions were stable with seeing about 1″. To reduce the effects of differential atmospheric dispersion, all Mars scans were guided through a Schott RG-5 filter so that the effective guiding wavelength was about 6500 Å.

Equivalent widths for the Martian water vapor lines were measured by methods described earlier. Assuming a temperature of 225 K, Voigt profiles and a value of $a = 0.05$ corresponding to a surface pressure of 6 mb; these equivalent widths were converted into total abundances of precipitable water by using water line strengths at 225 K given by Farmer (1971) and the tables of Jansson and Korb (1968). Using methods presented by Woodman and Barker (1973), airmass value for each observation was calculated from Martian physical data and estimates of atmospheric seeing during each observation. This method and its computer program were slightly modified to work with photoelectric data, and proved very informative as to different values of the airmass near the terminator (~ 5.0) and limbs (~ 2.8) of Mars due primarily to large phase angles ($\sim 45°$) for Mars.

A typical days' set of observations is shown in Figure 8, along with a diagram indicating spectrograph slit placement on the disk of Mars. Measured and calculated

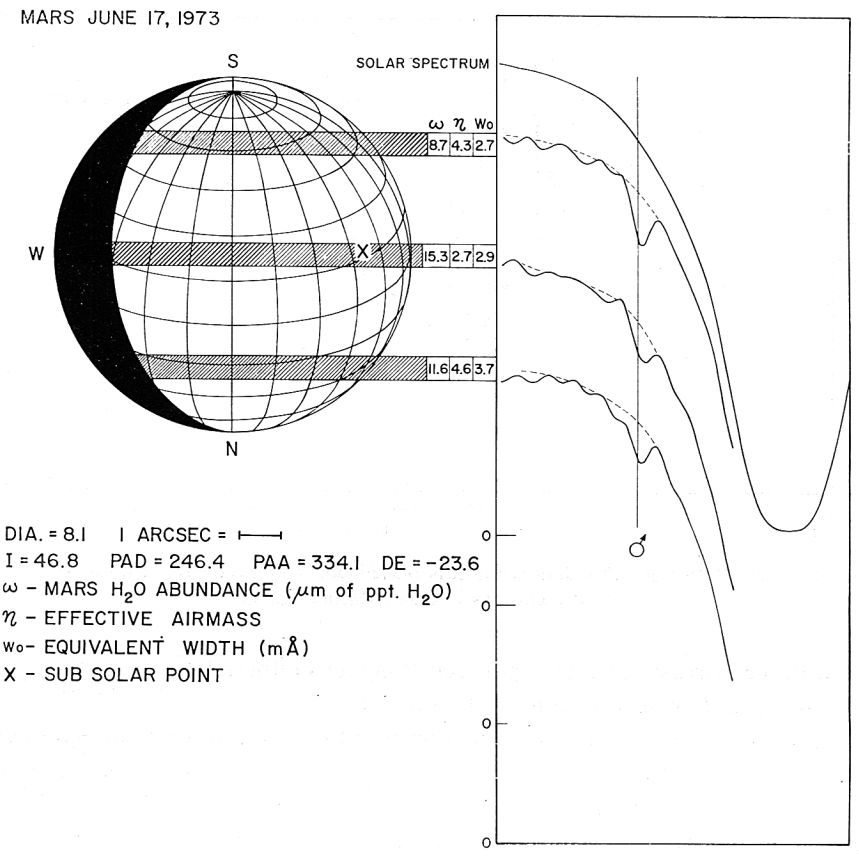

Fig. 8. Spectral scans of the 8176 Å line and slit positions for Mars on June 17, 1973.

values of the airmass, abundance and equivalent width are given for each slit position. Note that the smaller airmass nearer the center of the disk, unlike the airmass at 1.5″ from the polar limbs, more than compensates for the larger equivalent widths on the polar scans, resulting in a vertical equatorial abundance which is 50% greater than vertical polar abundances.

We can divide the 1972–73 data into three sets: PPCM (pole-to-pole on the central meridian), EQ (parallel to Mars equator) at various latitudes, and TERM (parallel to the terminator line) at positions near the limb and terminator and at the center of the disk. The various slit positions used are explained in the captions for Figures 9, 11, and 15.

Figure 9 is similar to Figure 7 but contains only 1972–73 data over the L_s range $126° < L_s < 270°$. The water vapor abundance seen along an entire central meridian quickly declines from a maximum of 25–40 μm near the start of the observations to a nearly constant level of 10–20 μm at an $L_s = 180°$. Then it continues to decline more slowly to a level of 6–10 μm up to $L_s = 250°$. The two relatively high PPCM observations after $L_s = 250°$ probably reflect real increases in planet-wide abundance asso-

https://doi.org/10.1017/S0074180900025456 Published online by Cambridge University Press

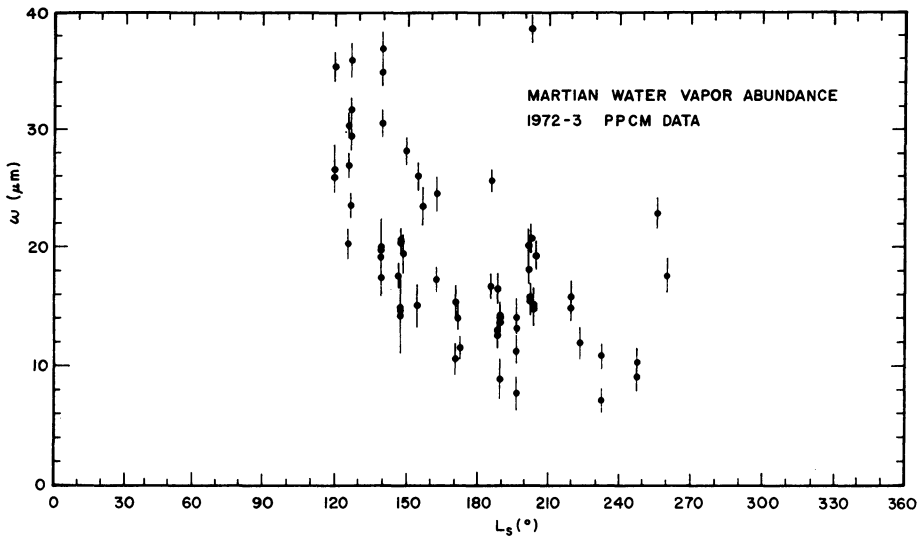

Fig. 9. 1972–73 Mars H_2O abundances for slits placed pole-to-pole on the central meridian as a function of Martian season, L_s.

ciated with the increase in water vapor seen at higher southern latitudes at the L_s values greater than 250° (see next section and Figure 11).

The conclusion can be drawn from Figure 9 that the atmospheric H_2O average over the entire planet decreased to a very low level of 8–10 μm around $L_s = 170°$ to 250°. So low a level could not have been measured before the use of the échelle coudé scanner, previous upper limits or detection limits based on high-dispersion spectrographic plates being in the range of 20 μm. The scatter in points is indicative of external errors or effects, since the typical internal errors are only of the order of one to two microns. In particular, the scatter may be representative of local weather or topography on Mars. To check the effect of topography and gravity variations, the data shown in Figure 9 are presented as a function of the central meridian longitude (L_{CM}) in Figure 10. No pronounced correlation can be noted with respect to L_{CM}, but a future analysis of the data will try to remove the effects of topography and gravity anomalies from the seasonal data.

Tull (1970) found, at $L_s = 132°$ and 148°, a north-south latitude distribution of water vapor abundance decreasing from a maximum in the north to a minimum in the south. The northern cap had just finished its regression and had reached its minimum area. The 1972–73 data which can be analyzed for latitudinal distribution were taken later in the Martian season than Tull's study. When plotted vs L_s in Figure 11, the equatorial data or latitudinal data show the same general decrease in abundance as the pole-to-pole or central meridian data until L_s reached 250°; when plotted vs L_{CM} we again find little indication of water vapor variation with longitude. But when the equatorial data are plotted as a function of Martian latitude, we see definite trends in the data for different seasons or values of L_s. Equatorial data can be broken into three

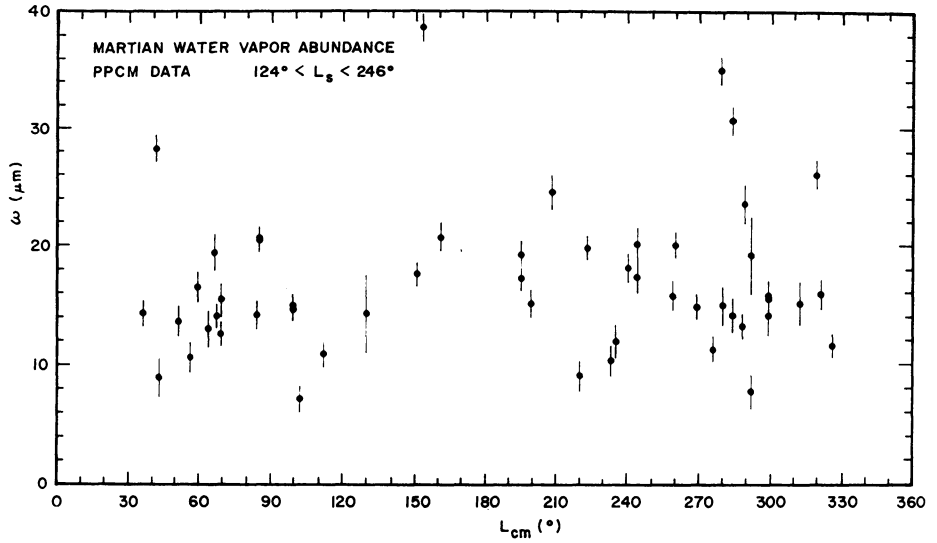

Fig. 10. 1972–73 Mars H_2O abundances for slits placed pole-to-pole on the central meridian as a function of central meridian longitude, L_{CM}.

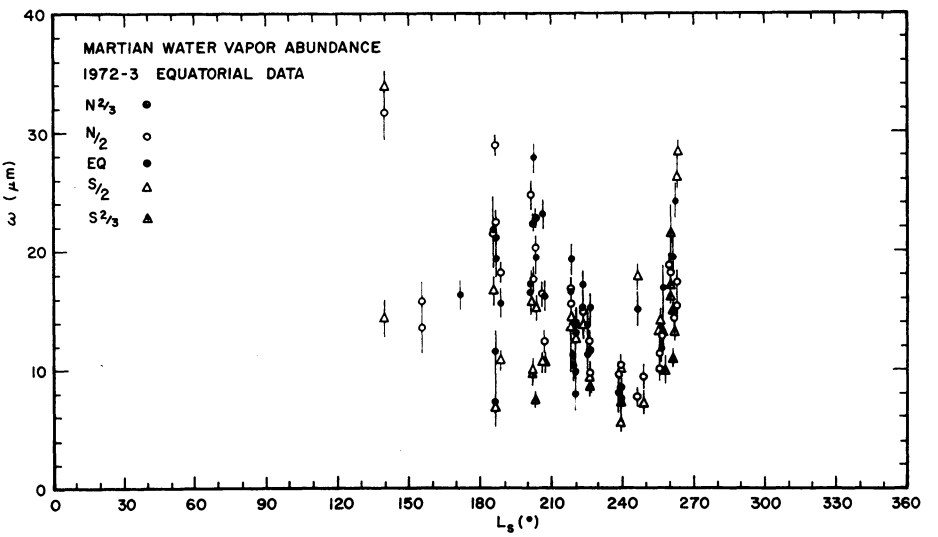

Fig. 11. 1972–73 latitudinal abundances of Mars water vapor as function of Martian season, L_s. Slit orientations are parallel to the Martian equator at various fractions of the disk diameter toward the poles; N2/3, N/2, EQ, S/2, and S2/3.

ranges of L_s, $185° < L_s < 208°$ and $217° < L_s < 249°$, which are plotted in Figure 12. The first period shows the same kind of N–S distribution found by Tull (1970) at earlier seasonal dates, $L_s = 132°$ and 148°. The second period has lower abundances with the decline in water occurring mostly in the northern and subsolar latitudes; the amount near the south polar cap (the surface area of which continues to shrink until $L_s = 270°$)

https://doi.org/10.1017/S0074180900025456 Published online by Cambridge University Press

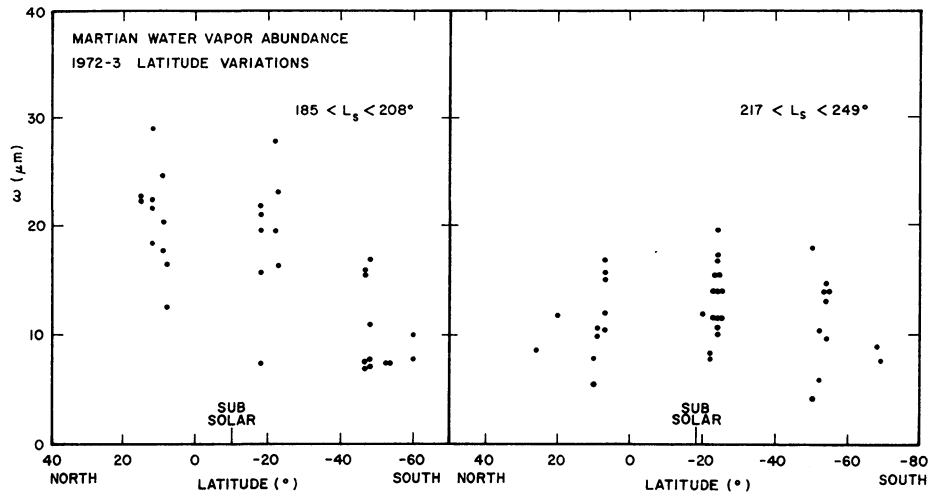

Fig. 12. 1972–73 latitudinal abundances as function of aerographic latitude for $185° < L_s < 208°$ and $217° < L_s < 249°$. Subsolar indicates the mean latitude or declination of the Sun as seen from Mars for this range of L_s.

remaining the same. The abundance over the subsolar latitude may be slightly higher, but a large scatter is also present at this latitude.

It is interesting to note that abundance at the edge of the south polar cap (at a latitude between $-60°$ and $-69°$) does not show any change between $L_s = 202°$ and $L_s = 239°$, over one seasonal month on Mars, indicating that the polar cap between $-60°$ and $-69°$ must be almost entirely solid CO_2 and not a solid CO_2–H_2O mixture.

The next range of L_s, $256° < L_s < 266°$, Figure 13, shows that around summer solstice, as the south polar cap is receding to its remnant size near $-80°$ latitude, the water vapor abundance increases markedly at middle southern latitudes, but those taken on the same dates at the edge of the cap show only a small increase.

Attempting to find out how water vapor behaves on a diurnal basis in the Martian atmosphere, we have obtained several sets of scans of three localities which represent the diurnal temperature variation on the Martian disk. By placing the spectrograph slit parallel to the terminator line near the terminator and limb (1.5″ onto the illuminated disk) and at the center of the disk as in Figure 14, we sampled areas each having roughly its own local Martian time and hence diurnal temperature phase. (Ideally, one should break the slit length down into smaller increments, but the signal level was not high enough to do so; consequently there is a temperature gradient along the slit length and possibly a seasonal effect with respect to latitude as discussed in the previous section.)

Due to the large phase angle of about 45° during the observing period, the subsolar point was under the limb scan most of the time. Slit positions refer to the following times during a day; Limb – midday, CD – mid-afternoon, and Terminator – late evening. Results of these sets of scans are presented in Figure 15 for three ranges of L_s in order to minimize any seasonal effect. Results are similar for the three periods

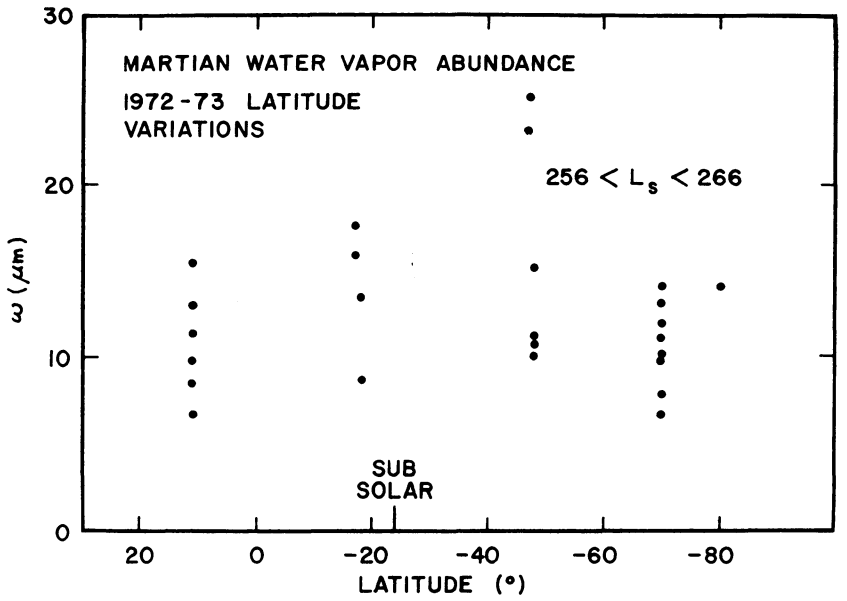

Fig. 13. 1972–73 latitudinal abundances as function of aerographic latitude for $246° < L_s < 266°$. Subsolar indicates the mean latitude or declination of the Sun as seen from Mars for this range of L_s.

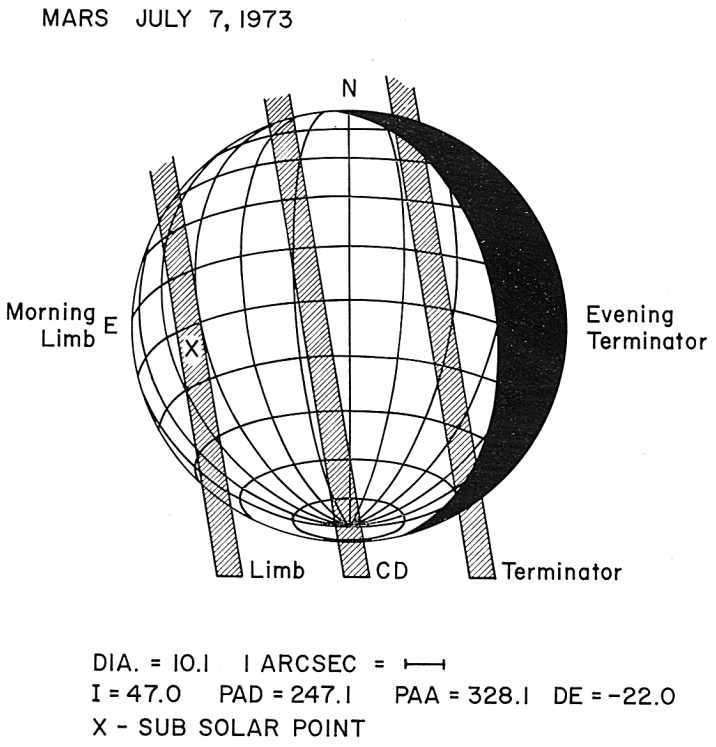

Fig. 14. Schematic representation of slit positions for diurnal data.

https://doi.org/10.1017/S0074180900025456 Published online by Cambridge University Press

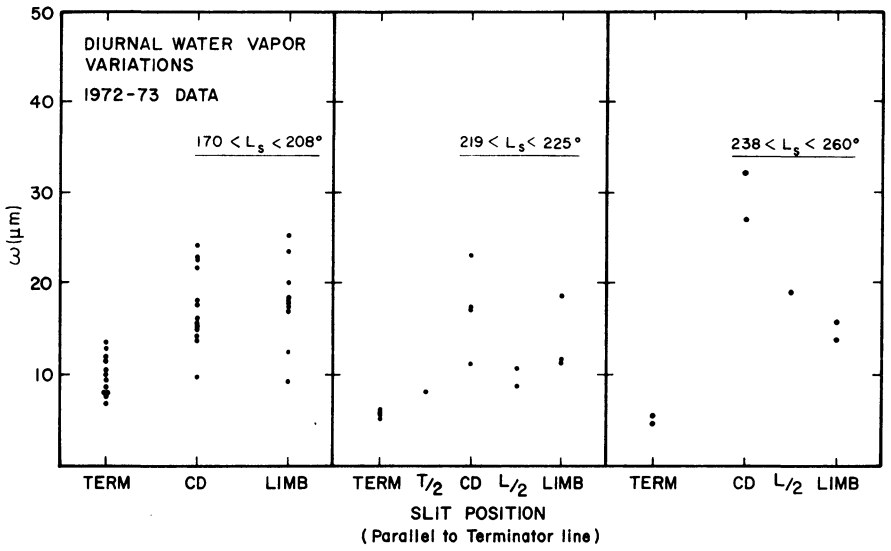

Fig. 15. 1972–73 diurnal water vapor abundances for $170° < L_s < 208°$, $219° < L_s < 225°$, $238° < L_s < 260°$. Slit orientations are perpendicular to the intensity equator at various fractions of the illuminated disk; TERM – terminator, T/2 – half way to the terminator, CD – center of the disk, L/2 – half way to limb, LIMB.

of L_s. The calculated airmass factor plays an important role in determination of water vapor abundance for these slit orientations. The limb and center of the disk values are similar because of their symmetry around the subsolar point and the sub-earth point, but the terminator airmass values can be quite large with 5.0 being a typical value. As the seeing improves, the airmass value increases because of lack of smearing which would bring more regions of lower airmass than higher airmass under the slit.

One definite conclusion can be drawn: the amount of water vapor near the evening terminator is smaller by a factor of two or more; water condenses out of the atmosphere as daytime temperature drops. The center-of-the-disk and limb abundances are not significantly different, probably due to the similarity between mid-day and early afternoon (time of maximum heating) temperatures. These diurnal variations need to be observed under the opposite orbital conditions of an evening limb and morning terminator. But from the data presented, we can plausibly infer that the amount of atmospheric water vapor is probably very small at sunrise, reaches a mid-day maximum, and is condensing out rapidly by late afternoon. This statement must be taken with the caution that these results refer only to the low water vapor abundance period of $170° < L_s < 260°$ and not necessarily to times of the Martian year when much larger amounts are present in the atmosphere, $L_s \sim 130°$ and $\sim 330°$.

Although water abundance seems to vary with many spatial parameters, an investigation was made into the assumption of an effective temperature of 225 K for water vapor. Four lines of differing strengths were used and scans were made in the EQ slit

position to minimize any topographical, local and diurnal variations. Abundances were calculated by using the line strengths given by Farmer (1971) for 200, 225 and 250 K. Using lines at 8176, 8181, 8234, and 8282 Å, observations were obtained at $L_s = 225°$. Another set was obtained at $L_s = 123°$ using the lines at 8176, 8189, and 8197 Å. The sigma for the rms fit of determined abundances indicated that at L_s of 123° the best temperature was 250 K; and similarly at $L_s = 220°$, $T = 200°$; and $L_s = 225°$, $T = 225$ K. The fit was not significantly better for any temperature; this indicates the method is not very sensitive when only a few lines are used and the abundance is low due to seasonal effects.

5. Conclusions

The new Mars water data, obtained during the first half of the 1973 apparition and presented here, represent more than three times the number of previous determinations of water vapor from all observers, and the internal error of each point is only about a third of that characteristic of the older photographic data because of sharply increased spectral and spatial resolution plus photon-counting photometry. Also, observations during a very important and previously unobserved seasonal period between $150° < L_s < 230°$ showed that the water vapor decreased to a small but observable 5–15 μm level by an L_s of 180°. Studies of the latitudinal and diurnal water vapor distributions indicate the location of maximum and minimum abundances for this season are positively correlated with surface temperature variations.

Acknowledgements

The author wishes to express his thanks to Mr Michael Perry who assisted in obtaining the majority of the observations and Mrs Amber Woodman for computer processing the digital data into final spectrum plots. Discussions with Drs Robert Tull, Ronald Schorn, Harlan Smith, C. B. Farmer, and Mr Jerry Woodman in various areas were quite useful. This work was supported by NASA NGR 44-012-152.

References

Barker, E. S.: 1971, *Bull. Am. Astron. Soc.* **3**, 277 (abstract).
Barker, E. S.: 1973, *Bull. Am. Astron. Soc.* **5**, 300 (abstract).
Barker, E. S. and Schorn, R. A.: 1973, *Bull. Am. Astron. Soc.* **5**, 301 (abstract).
Barker, E. S., Schorn, R. A., Woszczyk, A., Tull, R. G., and Little, S. J.: 1970, *Science* **170**, 1308.
Baum, W. A.: 1973, personal communication.
Baum, W. A. and Martin, L. J.: 1973, *Bull. Am. Astron. Soc.* **5**, 296 (abstract).
Farmer, C. B.: 1971, *Icarus* **15**, 190.
Fink, U., Larson, H. P., Kuiper, G. P., and Poppen, R. R.: 1972, *Icarus* **17**, 617.
Hanel, R., Conrath, B., Hovis, W., Kunde, V., Lowman, W., McGuire, E., Pearl, J., Pirraglia, J., Prabhakara, C., and Schlachtman, B.: 1972, *Icarus* **17**, 423.
Hunt, G. E.: 1972a, *J. Quant. Spectrosc. Radiat. Transfer* **12**, 405.
Hunt, G. E.: 1972b, *Bull. Am. Astron. Soc.* **4**, 360 (abstract).
Jansson, P. A. and Korb, C. L.: 1968, *J. Quant. Spectrosc. Radiat. Transfer* **8**, 1399.
Kunde, V. G.: 1973, *Bull. Am. Astron. Soc.* **5**, 297 (abstract).

Larson, L. P., Fink, U., and Michel, G.: 1973, *Bull. Am. Astron. Soc.* **5**, 297 (abstract).
Margolis, J. S. and Hunt, G. E.: 1972, *Bull. Am. Astron. Soc.* **4**, 359 (abstract).
Moroz, V. I. and Ksanfomaliti: 1972, *Icarus* **17**, 408.
Moroz, M. Ya. and Petrov, G. I.: 1973, *Icarus* **19**, 163.
Owen, T.: 1969, *Astrophys. J.* **150**, 121.
Owen, T. and Mason, H. P.: 1969, *Science* **165**, 893.
Rank, K. H., Fink, U., Foltz, J. V., and Wiggins, T. A.: 1964, *Astrophys. J.* **140**, 366.
Schorn, R. A. and Barker, E. S.: 1973, *Bull. Am. Astron. Soc.* **5**, 300 (abstract).
Schorn, R. A., Barker E. S., Gray, L. D., and Moore, R. C.: 1969, *Icarus* **10**, 98.
Schorn, R. A., Farmer, C. B., and Little, S. J.: 1969, *Icarus* **11**, 283.
Schorn, R. A., Spinrad, H., Moore, R. C., Smith, H. J., and Giver, L. P.: 1967, *Astrophys. J.* **147**, 743.
Spinrad, H., Munch, G., and Kaplan, L. D.: 1963, *Astrophys. J.* **137**, 1319.
Traub, W. B. and Carleton, N. P.: 1973, *Bull. Am. Astron. Soc.* **5**, 299 (abstract).
Traub, W. B. and Carleton, N. P.: 1974, this volume, p. 223.
Tull, R. G.: 1970, *Icarus* **13**, 43.
Tull, R. G.: 1972, in S. Iaustsen and A. Reiz (eds.), *Proc. ESO/CERN Conference on AuxiliaryInstrumentation*, Geneva, p. 259.
Tull, R. G. and Barker, E. S.: 1972, *Bull. Am. Astron. Soc.* **4**, 372 (abstract).
Wells, D.: 1972, *Publ. Astron. Soc. Pacific* **84**, 203.
Woodman, J. H. and Barker, E. S.: 1973, *Icarus*, **19**, 327.
Young, L. D. G., Young, A. T., Young, J. W., and Bergstralh, J. T.: 1973, *Astrophys. J.* **181**, L5.